Supporting Information

Dastjerdi et al. 10.1073/pnas.1017098108

SI Methods

Emphasis on Gamma Band Activity. We quantified the degree of gamma power (GP) change within an electrode by using the relative GP (RGP) values, which reflect the magnitude of GP change relative to its overall mean GP (OMGP) during the entire experiment. Although the change of electrophysiological activity could be measured within different narrow bands or with a broadband shift of power (1, 2), we focused our analysis on the changes in power within 30–180 Hz—i.e., broad (low and high) gamma band activity—for the following three reasons: (*i*) The task-dependent fluctuations of power within this band of activity are traditionally used in electrocorticography (ECoG) studies and are known to correlate reliably with underlying neural activity (2–7); (*ii*) this band of activity has spatially specific signal, whereas lower frequency bands exhibit changes over a wider spatial area (8); and (*iii*) there is already a wealth of evidence linking this band of activity with the hemodynamic signals detected during fMRI studies (9, 10).

To ensure that the lower edge of the selected gamma range was not affecting estimates of power change, we also conducted our analysis using an 80- to 180-Hz range. This range showed a similar significant but lower negative correlation ($r = -0.2$, $P < 0.001$) between relative gamma response for math and rest conditions. This finding suggests that the broader gamma range used in our analysis contains relevant task-related information. Typically, the PMC shows a spectral peak in the theta range of 5–7 Hz; however, some non-PMC sites were peaked at higher frequencies. Apart from two electrodes in one subject, we had no sites with spectral peaks of >15 Hz (the two exceptions showing a 20-Hz peak at motor cortex). Therefore, the gamma band used did not include oppositional changes in low-frequency spectral peaks that would lower estimates of gamma response and possibly task sensitivity.

Experimental Stimuli. Math stimuli were as follows: "8 + 65 = 73", "51 + 6 = 57", "68 + 7 = 75", "9 + 23 = 34", "47 + 8 = 55", "54 + 4 = 58", "38 + 6 = 42", "5 + 87 = 92", "28 + 6 = 34", "1 + 41 = 42", "61 + 2 = 63", "31 + 8 = 39", "20 + 4 = 24", "45 + 9 = 54", "33 + 5 = 38", "29 + 4 = 33", "81 + 5 = 86", "6 + 39 = 47", "46 + 3 = 49", "78 + 2 = 80","2 + 60 = 72", "7 + 43 = 50", "3 + 89 = 94", "8 + 30 = 38", "4 + 25 = 29", "24 + 5 = 29", "82 + 8 = 90", "26 + 7 = 34", "59 + 7 = 66", "42 + 6 = 48", "9 + 86 = 95", "6 + 36 = 42", "4 + 49 = 53", "5 + 63 = 68", "27 + 3 = 30", "2 + 52 = 56", "48 + 7 = 65", "1 + 18 = 19", "32 + 8 = 40", "3 + 75 = 78", "44 + 9 = 53", "7 + 34 = 42", "16 + 8 = 24" "50 + 9 = 59", "58 + 3 = 61", "6 + 22 = 28", "77 + 4 = 83", and "56 + 9 = 65".

Self-referential autobiographical stimuli were as follows: "I wore white socks yesterday", "I ate pizza this week", "I used a computer today", "I ate breakfast today", "I made my bed this morning", "I was on a highway today", "I drove a car today", "I ate a fruit today", "I read a book this week", "I ate at a restaurant this week", "I had chicken for dinner yesterday", "I watched TV today", "I went shopping this week", "I drank coffee this morning", "I talked on the phone today", "I took a shower this morning", "I went to the movies this week", "I read a newspaper today", "I spent money today", "I listened to music today", "I washed dishes yesterday", "I talked to a relative this morning", "I wore jeans yesterday", "I slept well last night", "I woke up early this morning", "I listened to the radio today", "I went to bed early last night", "I took a nap today", "I cooked dinner last night", "I went dancing this week", "I went to the beach this week", "I read a book this week", "I watched a sports game this week", "I went swimming this week", "I checked my email this morning", "I played with a dog this week", "I bought a CD this week", "I ate a burrito this week", "I went to the mall this week", "I drank juice this morning", "I went on a walk today", "I rented a movie this week", "I read a magazine yesterday", "I ate candy yesterday", "I went to the bank yesterday", "I played a video game this week", "I worked out this week", "I did my laundry this week".

Self-internal statements were as follows: "I am a quiet person", "I am an emotional person", "I am a loving person", "I am generous", "I am a relaxed person", "I am a good listener", "I am funny", "I am talkative", "I am polite", "I am honest", "I am competitive", "I am a patient person", "I am a quick learner", "I am friendly", "I am a moody person", "I am a happy person", "I am easily upset", "I am easily stressed", "I am a focused person", "I am easily distracted", "I am a demanding person", "I am very thoughtful", "I am very observant", "I am a confident person", "I am a curious person", "I am compassionate", "I am a nurturing person", "I am creative", "I am easily bored", "I am easily scared", "I am shy", "I am dependable", "I am kind", "I am outgoing", "I am helpful", "I am sensitive", "I am hard-working", "I am easily frustrated", "I am a silly person", "I am a caring person", "I am lazy", "I am a selfish person", "I am controlling", "I am a rude person", "I am respectful", "I am smart", "I am a serious person", "I am easily disappointed".

Self-external statements were as follows: "I usually wear white socks", "I eat pizza often", "I use computers often", "I usually eat breakfast", "I often make my bed", "I drive on highways often", "I drive a car", "I eat fruit often", "I read books often", "I eat at restaurants a lot", "I eat chicken often", "I watch a lot of TV", "I go shopping often", "I drink coffee often", "I talk on the phone a lot", "I take showers in the morning", "I go to the movies often", "I read the newspaper", "I spend a lot of money", "I listen to music often", "I wash dishes", "I talk to my family often", "I wear jeans often", "I am a deep sleeper", "I usually wake up early", "I listen to the radio", "I usually go to bed early", "I take naps often", "I usually cook dinner", "I dance often", "I go to the beach sometimes", "I read books often", "I watch sports games", "I swim sometimes", "I check my email often", "I have a dog", "I buy a lot of CDs", "I eat burritos often", "I go to the mall a lot", "I drink juice often", "I go on walks often", "I rent a lot of movies", "I read magazines", "I eat a lot of candy", "I go to the bank often", "I play video games often", "I work out a lot", "I do my laundry often".

Functional Imaging. Functional MR images were acquired on a 3T GE MRI scanner with a custom-built quadrature birdcage head coil. Functional MR images were acquired using a spiral-in/out pulse sequence (11) with the following parameters: one shot, TR = 2,000 ms, TE = 30 ms, flip angle = 77 °, FOV = 220 mm, in-plane resolution = 3.4375 mm × 3.4375 mm, slice thickness = 4 mm, and slice gap = 0.5 mm. Twenty-five axial-oblique slices covering the entire brain were prescribed approximately along the AC-PC plane. Initially functional data were motion corrected using MCFLIRT (12). Each subject's structural T1 image was skull-stripped using BET (13). Registration of functional images to high-resolution structural and standard space images was carried out with FLIRT, using 7 degrees of freedom (df) to register functional images to the subjects' high-resolution structural images and 12 df to register those high-resolution images to standard space using the MNI152_T1_2mm atlas. All registrations were manually inspected to ensure proper registration. Each functional image was preprocessed by masking out the nonbrain voxels, using a voxel-wise demeaning of the data and normalizing the voxel-wise variance. Preprocessed resting state functional data were

analyzed using independent component analysis (14) as implemented by MELODIC (Version 3.05) in the FSL software package (www.fmrib.ox.ac.uk/fsl). Dimensionality and number of extracted components were automatically estimated for each data set as detailed elsewhere (15).

Electrode Localization. After implantation of the electrodes, postoperative head computed tomography (CT) images were acquired and coregistered with the preoperative structural MRIs to accurately localize and visualize electrode positions. We used strips and grids made by AdTech Medical Instrument Corp. for electrocortical recording and stimulation in our subjects. These electrodes have the following parameters: 4-mm flat diameter contacts with 2.3-mm diameter of exposed recording area (4.15 mm^2) and interelectrode distance of 10 mm between the centers of two adjacent electrodes (i.e., only 7.7 mm edge-to-edge distance).

Presurgical T1-weighted 3D spoiled gradient recalled MRI data were aligned to AC-PC space by manually identifying the anterior commissure, the posterior commissure, and a third point in the midsagittal plane. The data were resampled to 1-mm isotropic voxels using a b-spline image interpolation algorithm from SPM5 (http://www.fil.ion.ucl.ac.uk/spm). Postsurgical CT images indicating the location of electrodes were aligned to the T1-weighted MRI images using a mutual-information algorithm, also implemented in SPM5. The electrodes were easily identified in the CT scans, and their locations were manually marked. These images were visualized using ITKGray, a segmentation tool based on ITKSnap (16). These electrode images were imported into the mrVista package (http://white.stanford.edu/software) and projected onto the 3D mesh renderings of the T1 anatomical images produced, on which the fMRI activation is displayed, thereby conserving the electrode to T1 anatomical image alignment. This method allowed us to construct 3D visualization of electrode locations relative to each patient's cortical anatomy within a few millimeters (< ~5 mm) in error. The accuracy of reconstructed electrode sites was also validated by digital photos obtained intraoperatively.

Electrophysiological Data Acquisition and Preprocessing. We recorded ECoG data at 3,051 Hz through a 128-channel recording system made by Tucker Davies Technologies. Off-line, we applied a notch filter at 60 Hz and its harmonics to remove power line noise. We also removed data from any electrodes with epileptic activity as determined by the patient's neurologist (J.P.). Before data analysis, all raw time series were inspected for additional artifacts or recording malfunction, with any corrupt data being excluded.

Once raw time series had been cleaned of dominant artifacts, the data were re-referenced by using a common average reference method. All clean channels were averaged to create a common mean time series that was subsequently subtracted from each individual time series as a reference. After digital referencing, each channel time series was decomposed into a number of bandpass-filtered time series. Using custom routines in Matlab (MathWorks), we filtered each channel by transforming each signal into the frequency domain and removing the power of signal outside each bandwidth of interest (using a Gaussian window). We used 42 center frequencies logarithmically spaced between 1 and 250 Hz with a range of ±10% bandwidth. After bandpass filtering, the data were returned to the time domain via an inverse Fourier transform and down-sampled to 436 Hz.

ERSP. To visualize electrophysiological response, we created ERSP maps based on the normalized power of electrophysiological activity during each condition. A Hilbert transform was applied to each of the 42 bandpass-filtered time series to obtain instantaneous amplitude and power (17). Finally, power at each frequency was scaled by the total mean power to compensate for the skewed distribution of power values. Using the Hilbert-transformed time series, time-frequency analysis was performed for event-related data. We logged the onset and duration of each trial via photo diode event markers for each experimental condition time-locked with the ECoG recording. Event markers were used to align and average power at each frequency band over repeated trials for each condition to create ERSP maps.

We estimated the distribution of power for each frequency band by performing comparisons with surrogate data. First, we transformed the instantaneous power into the Fourier domain and added random phases, resulting in a surrogate of instantaneous power that has randomized phase but preserved amplitude. Therefore, the first- and second-order moments of the surrogate remained uncharged, but its local temporal structure was removed (18). A "null" ERSP was then constructed from the surrogate data with the same number of trials (randomly selected) as the condition of interest. This process was repeated 500 times to sufficiently estimate the mean and SD of the null ERSP. Finally, we standardized the original ERSP by subtracting the mean and dividing by the SD of the null ERSP to obtain z scores. The ESRP maps were used primarily to visualize the pattern of activity during a given condition. We relied on the statistical analysis noted below to measure the magnitude and significance of changes in activity.

DAI and Relative GP. As a means to assess the magnitude of response across all electrodes for conditions of interest, a simple index of power change was evaluated for each electrode and ranked. Changes in broad gamma band power were used for estimating electrode response as discussed below, although the method is applicable to any band of interest. Initially, signals were filtered by using an FIR filter (eegfilt; EEGLAB; http://sccn.ucsd.edu/eeglab/) with a bandpass over the gamma range from 30 to 180 Hz. As with the ERSP method above, a Hilbert transform was then used to obtain instantaneous power for the entire band. The average of power for each electrode, regardless of conditions, was then calculated to define an overall mean GP level. For condition-specific responses, event markers were used to identify and calculate the mean power for each condition by concatenating all relevant trials. To exclude the transient responses to the stimulus onset, estimates of average power started from 500 ms after stimulus presentation to the end of trial for the given condition.

To compare different electrodes from different subjects, we defined the DAI for each electrode by calculating the difference of GP in the condition from overall mean GP and dividing it by their sum. DAI values were averaged over all blocks (experimental sessions) for each electrode. As noted above, the rest condition was 5 s long, and the mean reaction times of response in nonrest conditions were 4.3 ± 2.45 s for the math and 2.3 ± 0.98 s for the autobiographical conditions. For the comparison of DAI values across conditions as shown in Fig. 5*A*, a bootstrapping method was used to account for the unbalanced number of electrodes constituting PMC (17) and non-PMC (98) groups. DAI values from the non-PMC group were resampled to match the PMC group sample size, and the mean and SD were calculated. This resampling was repeated 50 times to estimate the mean and SD of the DAI for the non-PMC group.

Response Onset Latency Time. In conjunction with the DAI, the same gamma band of instantaneous power was used to estimate response timing over electrodes. To quantify response timing, event markers were used to epoch instantaneous power from 200 ms before stimulus presentation to the end of each trial of interest. Each epoch of instantaneous power was smoothened by convolving with a balanced Gaussian window (sum = 1, std = 68 ms, width = 2.5 std). A trace was defined as responding to the stimulus if it passed an arbitrary threshold (≥1.5 multiplied by overall mean GP) and remained above that threshold for 100 ms (approximately three cycles of the lower edge of gamma band; 30

Hz). For each responding trace, a window from 200 ms before and 100 ms after the trace passed threshold was divided into 20-ms nonoverlapping bins, each fitted with a least-squares line to estimate trace slope. Slopes were ranked (max-min) and the bin with the smallest mean square error from the top five ranked slopes was selected. The start time of the selected bin defined the response onset latency. An electrode was defined as responsive to a condition if at least 80% of traces (trials) were estimated to respond. The median latency and its error were then estimated for each electrode and condition of interest.

Because the latency depends on the threshold and the width of the smoothing function, we compared the obtained latency with a randomly generated latency. By using the same method mentioned above, response latency was estimated for randomly selected event epochs and repeated 50 times to estimate a median random latency. Median latency for real data was compared with the median of the random latency using a Wilcoxon rank test to establish that estimated response latencies were consistent across trials (i.e., latencies were not randomly distributed).

1. Miller KJ, Zanos S, Fetz EE, den Nijs M, Ojemann JG (2009) Decoupling the cortical power spectrum reveals real-time representation of individual finger movements in humans. *J Neurosci* 29:3132–3137.
2. Manning JR, Jacobs J, Fried I, Kahana MJ (2009) Broadband shifts in local field potential power spectra are correlated with single-neuron spiking in humans. *J Neurosci* 29:13613–13620.
3. Buzsaki G (2006) *Rhythms of the Brain* (Oxford University Press, London).
4. Jensen O, Kaiser J, Lachaux JP (2007) Human gamma-frequency oscillations associated with attention and memory. *Trends Neurosci* 30:317–324.
5. Lachaux JP, et al. (2005) The many faces of the gamma band response to complex visual stimuli. *Neuroimage* 25:491–501.
6. Crone NE, Miglioretti DL, Gordon B, Lesser RP (1998) Functional mapping of human sensorimotor cortex with electrocorticographic spectral analysis. II. Event-related synchronization in the gamma band. *Brain* 121:2301–2315.
7. Ray S, Crone NE, Niebur E, Franaszczuk PJ, Hsiao SS (2008) Neural correlates of high-gamma oscillations (60-200 Hz) in macaque local field potentials and their potential implications in electrocorticography. *J Neurosci* 28:11526–11536.
8. Canolty RT, et al. (2007) Spatiotemporal dynamics of word processing in the human brain. *Front Neurosci* 1:185–196.
9. Niessing J, et al. (2005) Hemodynamic signals correlate tightly with synchronized gamma oscillations. *Science* 309:948–951.
10. Logothetis NK, Pauls J, Augath M, Trinath T, Oeltermann A (2001) Neurophysiological investigation of the basis of the fMRI signal. *Nature* 412:150–157.
11. Glover GH, Law CS (2001) Spiral-in/out BOLD fMRI for increased SNR and reduced susceptibility artifacts. *Magn Reson Med* 46:515–522.
12. Jenkinson M, Bannister P, Brady M, Smith S (2002) Improved optimization for the robust and accurate linear registration and motion correction of brain images. *Neuroimage* 17:825–841.
13. Smith SM (2002) Fast robust automated brain extraction. *Hum Brain Mapp* 17: 143–155.
14. Beckmann CF, Smith SM (2004) Probabilistic independent component analysis for functional magnetic resonance imaging. *IEEE Trans Med Imaging* 23:137–152.
15. Greicius MD, Srivastava G, Reiss AL, Menon V (2004) Default-mode network activity distinguishes Alzheimer's disease from healthy aging: evidence from functional MRI. *Proc Natl Acad Sci USA* 101:4637–4642.
16. Yushkevich PA, et al. (2006) User-guided 3D active contour segmentation of anatomical structures: Significantly improved efficiency and reliability. *Neuroimage* 31:1116–1128.
17. Canolty RT, et al. (2006) High gamma power is phase-locked to theta oscillations in human neocortex. *Science* 313:1626–1628.
18. Theiler J, Eubank S, Longtin A, Galdrikian B, Farmer J (1992) Testing for nonlinearity in time series: The method of surrogate data. *Physica D* 58:77–94.

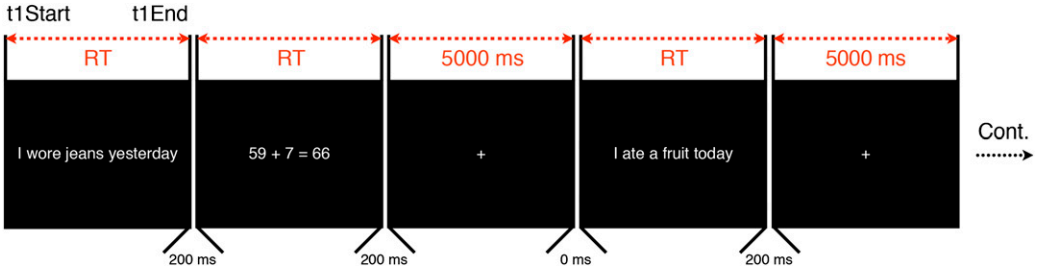

Fig. S1. Experimental task. We presented simple equations or sentences from different experimental conditions in random order while subjects were comfortably seated in bed. Subjects were asked to judge the accuracy of the sentence or math equation and to report their responses by pressing either "1" or "2" on a keypad corresponding to true or false, respectively. Subject's reaction time (RT) to each stimulus varied. The plus sign (rest condition) appeared randomly interspersed between task trials and remained on the screen for 5 s. The interstimulus interval (ISI) consisted of a blank screen shown for 200 ms (±20 ms), except during resting to nonresting trials where there was no ISI. Stimuli were presented in white font on a laptop screen with black background (oscilloscope measurements showed no flicker in the visible range, and the luminescence value was 95 cd/m^2). A similar version of this experimental task has been validated in fMRI studies of the DMN (1).

1. Kennedy DP, Courchesne E (2008) Functional abnormalities of the default network during self- and other-reflection in autism. *Soc Cogn Affect Neurosci* 3:177–190.

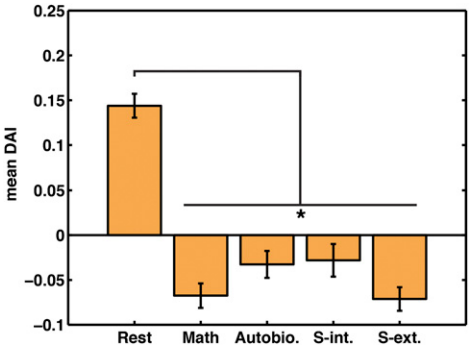

Fig. S2. Mean response for rest active electrode across all conditions (subject 2). Mean response for the PMC electrode shown in Fig. 2 was significantly different across presented conditions [$F(4, 453) = 28.79$, $P < 0.001$; one-way ANOVA], with the rest condition being significantly higher than all other conditions (*$P < 0.005$, Bonferroni corrected).

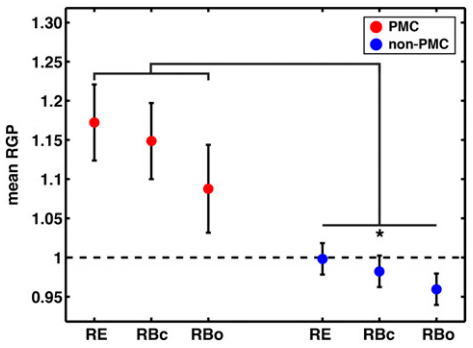

Fig. S3. RGP during resting events and blocks. The RGP during resting events (5 s of fixation, RE) is not significantly different from the RGP during resting blocks (3 min of resting) with either closed (RBc) or open eyes (RBo) for both PMC and non-PMC electrodes [$F(2, 651) = 1.2$, $P = 0.3$; two-way ANOVA]. However, there was a main effect of electrode location [$F(1, 651) = 24.2$, $P < 0.001$] with PMC electrodes having significantly different GP than non-PMC electrodes for all three conditions (*$P < 0.003$, Bonferroni corrected).

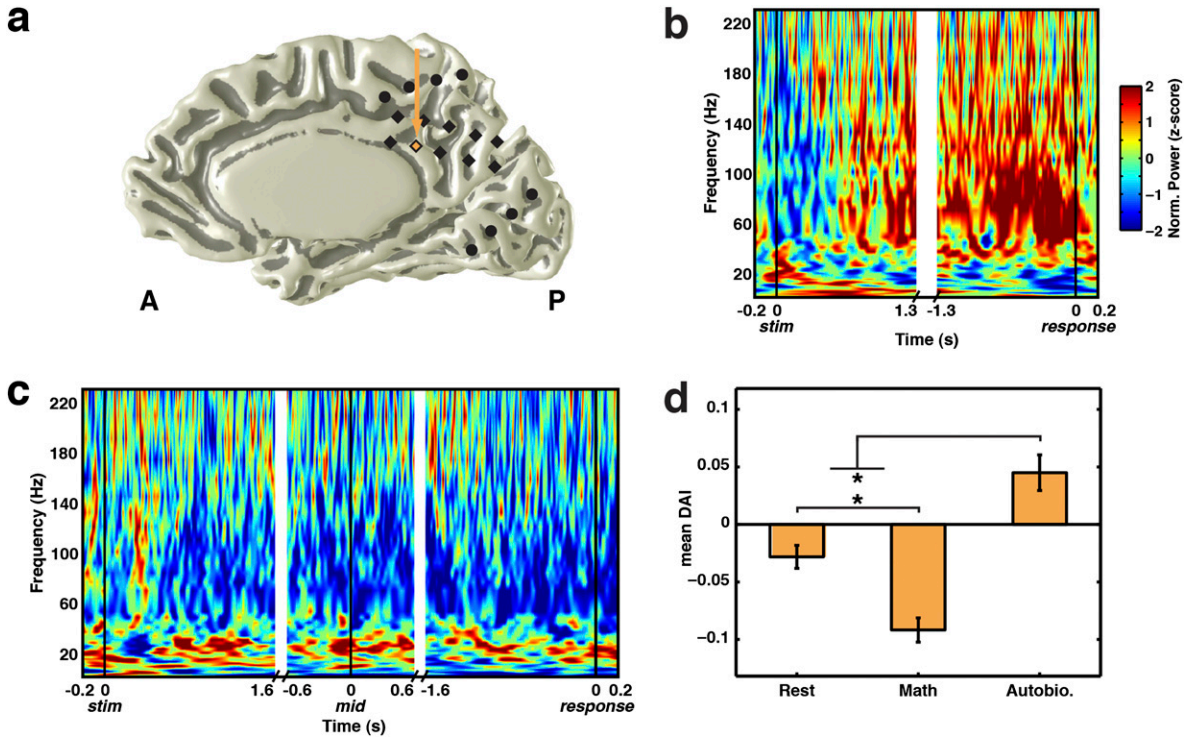

Fig. S4. PMC site responsive to autobiographical memory condition (subject 2). (*A–C*) ERSP plots for a PMC electrode (diamond) shown in *A* during autobiographical (*B*) and math (*C*) conditions. ERSP aligned as per Fig. 1. (*D*) The mean DAI for this electrode across all presented conditions. The mean DAI was significantly different across conditions [$F(2,261) = 31.48$, $P < 0.001$] with the autobiographical condition being significantly higher than rest and math conditions, which were also significantly different (*$P < 0.02$, Bonferroni corrected).

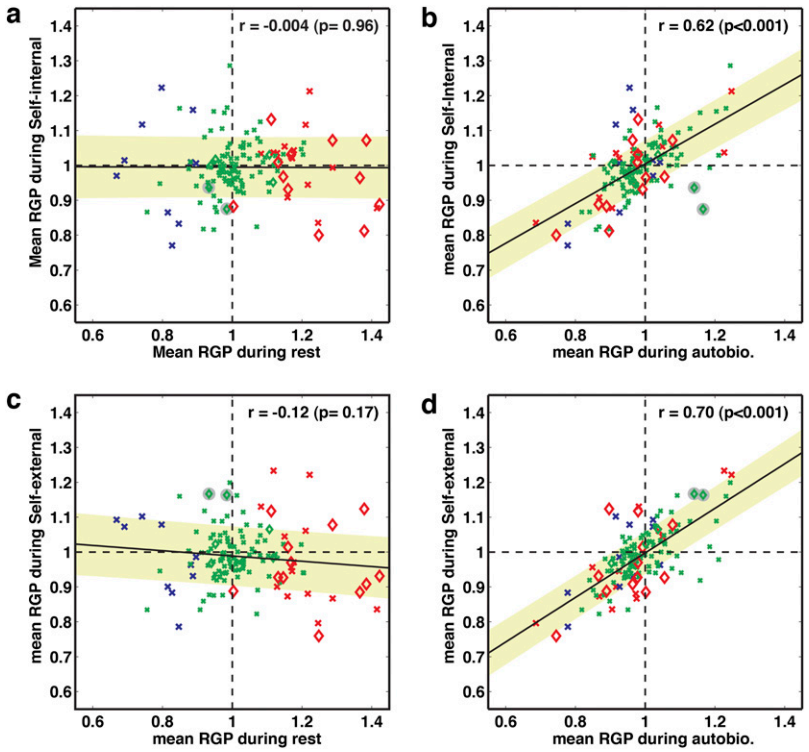

Fig. S5. Examining the correlation of gamma activity during rest and self-referential conditions. (*A–D*) RGP of each electrode during rest and autobiographical conditions is plotted against self-internal and self-external conditions including all electrodes from two subjects (subjects 1 and 2) across two experiments. The RGP during rest is not correlated with RGP during any of the self-referential conditions (*A* and *C*), whereas there is a significant correlation between RGP during autobiographical and other self-referential conditions (*B* and *D*). Gray markers in all plots denote electrode in Fig. 6. The solid black line with the yellow band shows the regression line with its SE.